The J. Exp. Biol. 208, 2661-2671
Published by The Company of Biologists 2005
doi:10.1242/jeb.01708

Spatial and temporal patterns of water flow generated by suction-feeding bluegill sunfish *Lepomis macrochirus* resolved by Particle Image Velocimetry

Steven W. Day[1,*], Timothy E. Higham[1], Angela Y. Cheer[2] and Peter C. Wainwright[1]

[1]*Section of Evolution and Ecology* and [2]*Department of Mathematics, University of California, One Shields Avenue, Davis, CA 95616, USA*

*Author for correspondence (e-mail: sday@alumni.virginia.edu)

Accepted 24 May 2005

Summary

The suction-feeding fish generates a flow field external to its head in order to draw prey into the mouth. To date there are very few empirical measurements that characterize the fluid mechanics of suction feeding, particularly the temporal and spatial patterns of water velocity in front of the fish. To characterize the flow in front of suction-feeding bluegill sunfish *Lepomis macrochirus*, measurements with high spatial (<1 mm) and temporal (500 Hz) resolution were taken using Particle Image Velocimetry (PIV). In an analysis separate from the PIV, high-speed video sequences were used for a novel method of visually tracking every seed particle for the duration of each feeding in order to determine directly the total parcel of water that the fish ingests. PIV measurements and particle tracking show that water is drawn from all around the mouth. Fluid velocity decreases rapidly with distance from the mouth and is only significant (>5% of speed at the mouth) within roughly 1 mouth diameter of the fish. Suction feeders gain little in terms of extending this flow field by even substantial increases in the fluid speed at the mouth opening. Instead, the chief advantage of increased flow speed at the mouth may be the increased magnitude of generated forces within the space very close to the mouth. After scaling of the velocity field based on size of the mouth opening and the measured fluid speed at a fixed position, the measured velocity profiles for all feedings are very similar to one another, so that a functional relationship for the magnitude of fluid speed as a function of distance from the predator mouth is presented and shown to be accurate over the range of kinematic variables tested. This relationship describes the velocity field both along the centerline of the fish and along transects lying at an angle to the centerline within both the mid-sagittal and frontal planes. Comparison of the time-resolved fluid velocity measurements to gape kinematics demonstrate that peak fluid speed occurs simultaneously with 95% of peak gape, showing that the bluegill maximizes nearly simultaneously both the generated forces and size of the region over which these forces act. The magnitude of peak fluid speed during each strike decreases as a function of increasing time to peak gape (r^2=0.87), demonstrating a strong relationship between the rate of buccal cavity expansion and maximum generated flow speed.

Key words: DPIV, suction feeding, Centrarchidae, sunfish, *Lepomis macrochirus*.

Introduction

Suction feeding is the most commonly used method of prey capture in fishes and many other aquatic feeding vertebrates. Within ray-finned fishes, the single biggest radiation of living vertebrates, suction-feeding morphology and behavior have undergone extensive diversification. Different species use various modifications of suction-feeding behavior to capture a vast variety of aquatic prey (Norton, 1991; Norton and Brainerd, 1993). Although the musculoskeletal basis of suction feeding in fishes has been studied intensively over the years (Aerts, 1990; Aerts et al., 1987; Carroll et al., 2004; Lauder, 1980b; Liem, 1973; Svanback et al., 2002), less attention has been paid to the patterns of fluid flow that are generated by suction feeders (Ferry-Graham et al., 2003; Lauder and Clark, 1984; Muller et al., 1982; van Leeuwen and Muller, 1984a). This fluid flow is central to the suction-feeding event because it imparts all of the forces that act to draw the prey into the predator's mouth. Suction-feeding success depends on the details of these water flow patterns and how the fish uses them to capture prey (Nyberg, 1971; van Leeuwen and Muller, 1984b; Weihs, 1980). Thus, a clear understanding of the fundamental time course of the suction flow and the spatial region over which it operates is required before the extensive morphological and behavioral diversity that exists among suction-feeding species can be fully interpreted.

During a suction-feeding event, the predator generates a flow of water by rapidly opening the mouth and expanding the buccal cavity. Prior work has modeled this flow using potential flow theory (Drost et al., 1988; Muller et al., 1982; Weihs, 1980) and

investigated the effects of ram/suction interactions using these inviscid irrotational models (van Leeuwen and Muller, 1984b; Weihs, 1980). Empirical measurements of this flow are rare, however, with only a single recent quantitative study (Ferry-Graham et al., 2003) providing measurements at select locations in a two-dimensional space in front of a feeding bluegill sunfish. All additional empirical studies are either largely qualitative (Muller and Osse, 1984; van Leeuwen and Muller, 1984a) or include quantitative measurements of particle streaking at select locations in front of the fish (Lauder and Clark, 1984). To date, no empirical study has resolved the flow field in front of the fish with sufficient spatial and temporal resolution to quantify the distribution of fluid speed as a function of distance in front of the fish. In this study we characterize the flow in front of suction-feeding bluegill sunfish *Lepomis macrochirus* by taking measurements with high spatial and temporal resolution using Particle Image Velocimetry (PIV) and a novel method of tracking individual seed particles for the duration of each feeding, to determine the parcel of water that the fish ingested.

The predator can manipulate the generated flow by modulating how wide the mouth is opened and also by varying the speed that it opens the mouth. This is the first empirical study to determine the effect of these kinematic variations on the flow field in front of the head, or to compare the relative timing of fluid speed to kinematic events. In this study we provide a quantitative functional description of the fluid velocity generated by suction-feeding bluegill sunfish and relate this flow pattern to the rate of mouth opening and the size of the mouth aperture.

By relating the timing of mouth opening to the temporal development of the flow field we are able to test one of the predictions from computational modeling studies of suction feeding. The expanding cone model of suction feeding was developed in the early 1980s and has provided the most complete insight to date of the coupling of internal expansion of the fish's head with the flow field generated by this expansion (Muller et al., 1982; van Leeuwen and Muller, 1983). A key result from this body of work was that peak flow speeds at the mouth aperture would be reached at a time relatively early in the gape opening sequence, at about 30–50% of maximum mouth diameter. We test this prediction.

Finally, we measured the volume of the ingested parcel of water to determine the shape of the water ingested by the fish and whether water exiting the opercular cavities posteriorly during the feeding sequence significantly contributes to the total water flow. To our knowledge there are no previous empirical measurements of the shape or volume of ingested fluid, although modelers have generated predictions of both variables in other fish species (de Jong et al., 1987; Drost et al., 1988; Muller and van Leeuwen, 1985).

Materials and methods

Experimental animals

Three bluegill sunfish *Lepomis macrochirus* Rafinesque, standard lengths 15.3, 15.0 and 15.4 cm, were used in this study. The fish were caught in Yolo county, near Davis, CA, USA and housed individually in 100 liter aquaria. The fish were fed daily a variety of squid (*Loligo*), live ghost shrimp (*Palaemonetes*), and annelid 'tubifex' worms. All fish maintenance and experimental procedures used in this research followed a protocol approved by the University of California, Davis Animal Care and Use Committee. Experiments were conducted in an aquarium dedicated to the experiments presented here. Each individual was moved from its housing aquarium to the experimental tank, where it remained until a sufficient number of quality high-speed video sequences were collected, at which point the individual was returned to its housing aquarium.

Experimental set-up

Digital Particle Image Velocimetry (DPIV) is a technique that measures the instantaneous velocity field within an illuminated plane of the fluid field using light scattered from particles seeded into the fluid (Adrian, 1991). Experiments were conducted in a 200 liter experimental aquarium that was integrated with a particle image velocimetry system (Fig. 1). An Innova I-90 continuous argon-ion laser rated at 5 W output power (Coherent, Inc., Santa Clara, CA, USA) and a set of cylindrical and spherical lenses created a collimated light sheet of approximately 1 mm thickness and 5–10 cm width, located within the aquarium. The laser sheet entered the bottom of the aquarium *via* a mirror and was directed upwards in the same orientation as the sagittal plane of the approaching fish. After traversing the tank a mirror near the surface of the tank reflected the sheet back down within the same plane as the upward directed beam, but angled towards the posterior of the fish. This downward-directed sheet illuminated the fluid field above and posterior to the upper lip of the fish, which would have been in the shadow of the upward-directed beam and also effectively doubled the amount of scattered light where both beams were present. The aquarium was seeded with 14 μm silver-coated glass beads (Potter Industries, Inc. Carlstadt, NJ, USA) with a specific gravity of 1.05. A NAC Memrecam ci

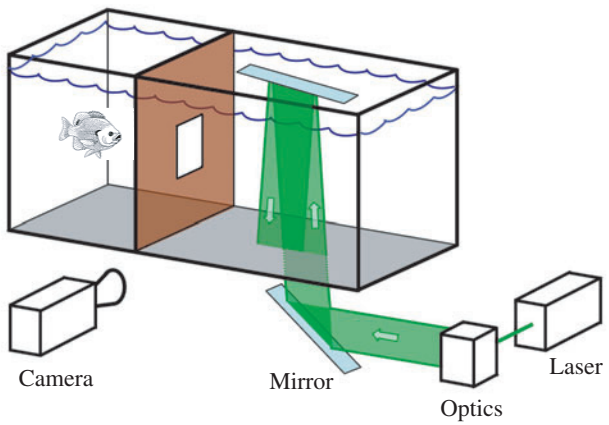

Fig. 1. Schematic of the experimental setup, showing experimental tank, position of laser sheet, optics, mirrors, camera, tank divider and door.

digital high-speed video camera (Tokyo, Japan) was used to acquire a lateral image of the fish and light scattered from particles. The camera has a 512×462 pixel CMOS sensor, and we used a frame rate of 500 Hz and a shutter speed of 1/3000 in order to reduce particle streaking at high fluid speeds.

Experimental protocol

Prey were positioned within the laser sheet and within the camera field of view. Although the bluegill swam freely during feedings, its mid-sagittal plane lay in the same plane as the laser sheet at the time of prey capture. An anterior view of the feedings was recorded at 30 Hz with a digital camcorder (Sony Inc., Tokyo, Japan) and used to determine the position of the fish within the laser sheet. Only measurements where the predator was centered on the laser sheet were analyzed. The high-speed video camera remained fixed in position and focused on the plane of the laser.

Prior to each feeding, the fish was confined to one end of the aquarium by a barrier and trap door. After opening the door, the fish was free to pass through a 5×15 cm opening in the barrier, which controlled the fish's starting position, to swim towards the prey (Fig. 1). Fish were fed both non-evasive (tubifex worms) and evasive (ghost shrimp) prey to elicit a range of effort. Worms were introduced through Tygon® tubing attached to a syringe and allowed to fall freely through the camera field of view. Live ghost shrimp were held in position by a thin (0.2 mm diameter) steel wire or surgical thread introduced under the exoskeleton. While controlling the initial position of the shrimp, tethering did not normally prevent the escape response of the prey. Every third shrimp introduced to the fish was not constrained in any way. While the unrestrained prey did not normally remain in the camera field of view or lead to successful measurements, they helped to sustain the effort of the bluegill. The total number of feedings for individuals 1, 2 and 3 were 16, 17 and 9, respectively. 23 of these were worm feedings and 19 were shrimp.

Feeding sequences where the prey remained within the laser sheet and camera field of view prior to the strike were kept for analysis. Images were transferred from NAC proprietary format into a series of TIFF images. The entire sequence from the beginning of mouth opening until mouth closure lasted for 20–150 images (40–300 ms), depending on the speed of the strike.

Data analysis

The positions of the anterior margin of the eye, anterior tip of the upper jaw and anterior tip of the lower jaw were measured for each image of the video sequence by manually tracking using Image J (NIH, Washington, DC, USA). These coordinates were copied into an Excel spreadsheet and used to calculate several kinematic variables. The position of the center of the mouth was defined as the midpoint between the upper and lower jaw tips. Gape was the distance from tip of the upper jaw to tip of the lower jaw and peak gape (*PG*) was the maximum value of gape during the strike. Time to peak gape (*TTPG*) was the duration from 20% of *PG* to 95% of *PG*, as in Sanford and Wainwright (2002). This was done to eliminate the highly variable stage that occurs during the beginning of mouth opening and because the exact time when peak gape is reached is difficult to determine accurately due to its asymptotic approach. Ram speed was calculated as the horizontal component of the temporal derivative of eye position. Jaw protrusion was the increase in distance from the center of the mouth to the eye referenced to the initial distance between these, and jaw protrusion speed was calculated as the time rate of change of this distance. The measurements of jaw protrusion and horizontal position were smoothed with a 3-point moving average before calculating derivative quantities. Derivatives were calculated as a two-point derivative approximation, which is justified in light of the fact that only the relative timing and not the magnitude of derivative quantities is relevant to the results.

An adaptive mesh cross-correlation algorithm created by Scarano and Riethmuller (1999) was used to calculate fluid velocities from image pairs, each pair consisting of two successive images from the high-speed video sequence. All of the measurements for this work used an initial interrogation window size of 64×64 pixels and two refinement steps. The final image interrogation used 16×16 pixel interrogation regions with 50% overlap, so that the measurement grid spacing was 8 pixels, corresponding to approximately 0.7 mm for the camera field of view (3.7×5 cm). Each image pair lead to a simultaneous measurement of two components of velocity at every location on a regularly spaced i,j ordered measurement grid with overall dimensions of i=53 and j=70. In addition to two components of velocity, the algorithm returned the signal-to-noise ratio (SNR) for each correlation in the final interrogation and this was used for validation of the measurements.

All measured and presented fluid speeds are in the earth-bound, or absolute, frame of reference. Fluid speeds along three transects radiating from the center of the fish's mouth were extracted from every two-dimensional vector field. This extraction of speed along all three transects of interest was automated with a custom program written in Visual Basic because the absolute position of the fish, and therefore positions of the transects vary during the strike. The program probed the PIV velocity data, accounting for both the angle of the fish and the position of mouth as determined from manual digitization.

Data validation

Cross-correlation-based PIV algorithms typically return an estimated speed at every grid point. Evaluating the accuracy of these measurements is complicated, but uncertainty generally increases as a result of poor seeding in that region of the image, high velocity gradients, solid boundaries that scatter light, and particle displacements that are large relative to the size of the interrogation region. In order to insure that only quality measurements were used, a two-step validation scheme was implemented.

First, vectors with a signal-to-noise ratio (SNR) of less than 2.0 were removed, without replacement, and no smoothing was applied to the final velocity field. Some spurious measurements that are not representative of fluid particle displacement still passed the SNR validation criterion. The second step of the validation scheme deals with these spurious vectors. Measurements both directly on the transect (i,j) and at two grid points above (i,j+2) and two grid points below (i,j–2) were considered at each horizontal position along the transect. Measurements located 2 grid points away from the primary measurement location are used because these do not overlap the primary measurement region. If at least two of the three measurements considered had not been removed based on the SNR criterion (step one of the validation scheme), then the mean of the remaining measurements was used as the value of speed for that given position along the transect.

This validation scheme resulted in the removal of some measurements near the mouth for all sequences. Measurements near the mouth were the most likely to fail the validation scheme because particle displacements (high fluid speed), velocity gradients, and occasional glare from the predator, were all highest near the fish mouth. The camera frame rate and spatial resolution used for the measurements placed an effective upper limit of measured fluid speed at approximately 1 m s^{-1}, corresponding to a 16 pixel displacement between images. For the majority of feedings, all measurements further than 2–3 mm from the mouth were validated and those further than 5 mm from the mouth were validated for all feedings.

A time series of extracted profiles of speed was inspected to determine the time of peak fluid speed for each feeding. The extracted transects at the time of peak fluid speed for multiple feedings were compared. To address the variation in size of velocity pattern with gape and the strike-to-strike variation in magnitude of fluid speed, profiles of scaled fluid speed were compared to one another. Based on either the physical intuition or the form of the equation for theoretical velocity along the centerline of the existing theoretical models (equation 25, Muller et al., 1982), it was reasonable to predict that the size of the spatial pattern scaled linearly with size of gape and that the magnitude of fluid speed everywhere would be proportional to fluid speed *FS* at the mouth aperture. For each feeding, the profile at the time of peak fluid speed was scaled by dividing spatial distances by gape at this time and the magnitude of speed by the measured speed located at a distance of $\frac{1}{2}$ gape in front of the fish. The speed at this position is used throughout as a reference because at this location fluid speed is substantial and the PIV measurements meet the validation criteria described above; it is referred to as $FS_{\frac{1}{2}\mathrm{gape}}$ from here on. Profiles at this time of the strike were selected because the high values of fluid speed occurring at the same time as large gape make this a biologically relevant portion of the strike.

After scaling, all data from extracted centerline transects for each individual were combined and a fourth order polynomial fit to the data was generated to create a functional representation of the mean scaled speed profile for that individual, $SS_{\mathrm{individual}}(x)$. The square of the correlation coefficient (r^2) of this curve fit was calculated to determine the quality of the fit. To quantify the strike-to-strike variation of scaled velocity profiles, measurements were binned together at equally spaced intervals (0.1 scaled distance) along the scaled distance axis and the residuals of all measurements within each bin about the polynomial fit were calculated in order to quantify the variation of the scaled velocity profiles about the mean scaled velocity profile.

In a subsequent analysis all of the data from the three individuals was combined to create one pooled data set. As was done for each individual, a polynomial fit was generated for the pooled data, $SS_{\mathrm{pooled}}(x)$, and residuals of measurements about this fit were binned to quantify the variation about this mean velocity profile. Additionally, for each individual, the r^2 of both the individual polynomial fit, $SS_{\mathrm{individual}}(x)$, and of the pooled data polynomial fit, $SS_{\mathrm{pooled}}(x)$, to the data subset consisting of all feedings for the particular individual were calculated and compared to one another. Lastly, in order to provide a preliminary evaluation of the theoretical model of Muller et al. (1982), the r^2 of the Muller centerline equation (equation 25 in Muller et al., 1982) to each individual's data subset and to the pooled data set was calculated. The theoretical equation was calculated with a mouth diameter of 1 and value of speed at the aperture of 2.83, which results in the same spatial scaling as was done with empirical measurements and a value of scaled speed of 1 at a scaled distance of 0.5.

For one individual the experimental setup was modified to obtain an additional set of measurements in a frontal plane. The same digitization, image processing and extraction of transects was conducted, although instead of using the true value of *PG* for each sequence a constant value (equal to the mean value of the sequences with a lateral view of the fish, 12 mm) was used because it was not possible to measure peak gape as defined here from the ventral view. The scaled speed profiles were again combined and used to determine mean velocity profiles for the three transects within the mid-frontal plane. All transects share a common intersection at the center of the mouth opening, lying within the plane of the mouth opening. These were compared to mean velocity profiles in the mid-sagittal plane in order to evaluate the symmetry of the flow field about the long axis of the fish.

In a separate analysis of the video sequences of particle motion, the parcel of fluid that was eventually ingested by the fish was determined by manually tracking individual particles. Any particle that entered the predator's mouth at any time between mouth opening and mouth closure was considered ingested. The result of this analysis was the definition of a boundary for which all fluid elements located within the boundary at the beginning of mouth opening were ingested by the fish. All elements lying outside the boundary were not ingested. The volume of this ingested parcel of water was calculated by integration of the two-dimensional boundary, assuming that the flow field is symmetric about the long axis of the fish.

Temporal pattern

The temporal pattern of kinematic events and fluid speeds was investigated by plotting gape, ram speed, jaw protrusion speed and fluid speed as a function of time for the duration of every strike. The relative timing of key kinematic events was determined manually from the graphed profiles of each feeding. These included start of mouth opening, gape equal to 20% peak gape, gape equal to 95% peak gape, start and finish of prey capture, and the time of peak fluid speed at three distances ($\frac{1}{4}PG$, $\frac{1}{2}PG$, PG) along the centerline transect of the fish. The interval between each of these and time of 20% peak gape was calculated as a fraction of the time from 20% peak gape to 95% opening (*TTPG*) as a first order approximation, accounting for the variation between fast and slow strikes. The mean and standard error (S.D.) of each scaled interval was calculated for all 42 feedings in order to determine the general pattern of the relative timing of events across individuals and for the entire range of *TTPG* reported.

In order to determine the effects of prey type, two-way analyses of variance (ANOVAs) were performed with prey type and individual as the independent variables and *TTPG*, $FS_{\frac{1}{2}PG}$ and *PG* as the dependent variables.

The peak fluid speed measured at a distance of $\frac{1}{2}$ peak gape in front of the fish, $FS_{\frac{1}{2}PG}$, was plotted as a function of measured time to peak gape, *TTPG*, for every feeding of each individual. A power line fit was applied to the feedings of each individual.

Unless otherwise stated, all results are mean ± standard deviation (S.D.).

Results

After a period of acclimation to the experimental tank and laser sheet, fish fed apparently unaffected by the laser sheet. There was substantial variation among feeding trials in both peak gape and speed of mouth opening (*TTPG*) for all individuals. *TTPG* ranged from 12 to 58 s and was strongly affected by prey type, with worm feedings (42±7 ms) being slower than feedings on ghost shrimp (20±7 ms). Peak gape ranged from 9.0 to 19.1 mm (12.1±1.9 mm for worms and 13.4±2.0 mm for shrimp) and was not significantly affected by prey type (P=0.36).

At all times during all strikes, the PIV measurements showed that the fluid affected by the suction-feeding fish was constrained to a region in close proximity to the mouth (Fig. 2). The area of significant fluid velocity formed a mushroom-shaped region extending approximately equal distances both forward and to the sides of the mouth. The magnitude of fluid speed decayed rapidly with distance in front of the fish, being approximately 25% the speed at the mouth at a distance of $\frac{1}{2}$ mouth diameter and 5% at a distance of 1 mouth diameter. Both the size of the affected region and magnitude of flow speed at the mouth were highest at a time corresponding to near peak gape. The fish began to ingest water when the mouth began to open and ingestion continued until mouth closing.

Spatial pattern

The spatial distribution of velocity was primarily dependent on gape and the magnitude of speed generated at the mouth, such that for a faster strike (low *TTPG*), or larger peak gape (*PG*), there was an increase in the generated fluid speed everywhere in front of the feeding fish (Fig. 3A). Scaling the spatial size by the mouth diameter at the time of peak fluid speed and magnitude of speed by fluid speed at a reference location located at a distance of $\frac{1}{2}$ gape in front of the fish ($FS_{\frac{1}{2}gape}$) for numerous feedings demonstrated similarity of the spatial pattern between individuals over the observed range of peak gape and *TTPG* (Fig. 3B). While profiles of absolute speed varied greatly from feeding to feeding, the scaled profiles were very similar to one another. A mean scaled velocity profile found by fitting of a fourth order polynomial

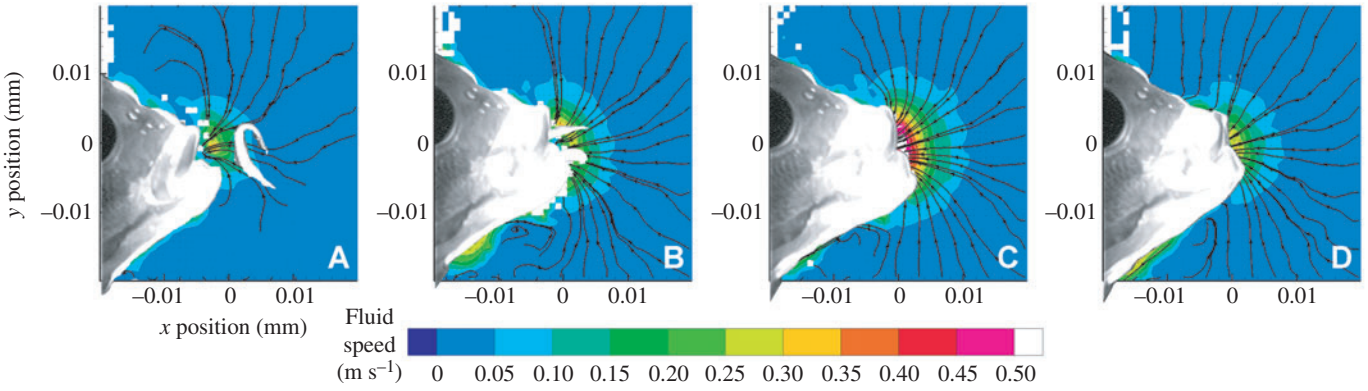

Fig. 2. Representative PIV measurements of the fluid field in front of the feeding fish at four times; opening (A), prey entering (B), peak gape (C), and closing (D) during the strike. Color contours represent the magnitudes of fluid speed and streamlines show the direction of velocity. The position of both the predator and prey are shown overlaid on the PIV measurement. Note that the region of significant fluid velocity induced by suction is constrained to a region in close proximity to the mouth and extends approximately equidistant in all directions from the mouth, and that the magnitude of speed and size of the affected region both increase during mouth opening and are maximum at peak gape. Measurements with a signal-to-noise ratio less than 2.0 are removed, but the more rigorous validation scheme that was applied to the extracted profiles has not been applied, resulting in some erroneous measurements near and within the mouth aperture in frames A and B.

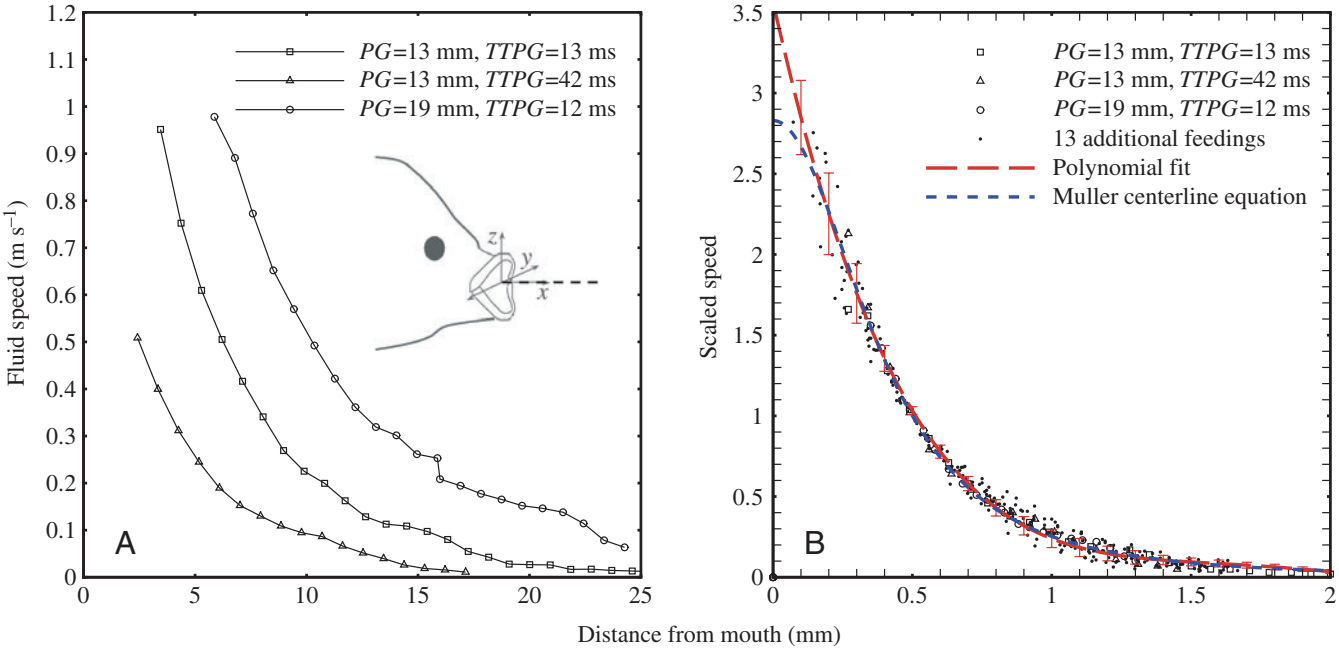

Fig. 3. Profiles of speed (A) and scaled speed (B) measured along the centerline transects for three different feedings of the same individual. (A) The magnitude and shape of the velocity profile are affected both by variation in peak gape (*PG*) and time to peak gape (*TTPG*). (B) Data for the same three feedings as in A, in addition to 13 others from this individual, after scaling. Spatial distances are scaled by gape at the time of the velocity measurement. Fluid speeds are scaled by the fluid speed measured at a distance of $\frac{1}{2}$ gape ($FS_{\frac{1}{2}gape}$) in front of the fish. A polynomial fit to the data of all 16 feedings is shown as a red broken line (r^2=0.986). Error bars represent the S.D. of the residuals about the fit line and are shown at every 0.1 scaled distance. The equation for speed along the centerline from the theoretical model of Muller (1982) is shown as the blue broken line (r^2=0.986). Note that although variations in *PG* and *TTPG* have a significant effect on the absolute values of speed, the scaled profiles for all transects are very similar to one another.

fit to the 42 pooled feedings from all individuals provided a good fit (r^2=0.985) to the scaled fluid centerline profiles from all feedings for this individual (#1), as shown in Fig. 2B. The S.D. of residuals of scaled fluid speeds about the mean scaled velocity profile are shown as error bars in Fig. 2B and can be seen to increase in magnitude towards the mouth. This is a result of both increased magnitude of the scaled speed and increased variation due to uncertainty in the measurement.

The equation of speed along the centerline of the fish predicted by the theoretical model of Muller et al. (1982) also provides a good fit (r^2=0.986) to the scaled centerline profiles from all feedings of this individual (#1), also shown in Fig. 3B, and to the entire pooled data set consisting of all 42 feedings from the three individuals (r^2=0.984). The mean scaled velocity profile along the centerline was very similar for each individual, as shown in Fig. 4. The polynomial fit to the pooled data set of 42 feedings (r^2=0.983), including all feedings from all individuals, was given as:

$$SS_{pooled} = 0.348x^4 - 2.49x^3 + 6.61x^2 - 7.78x + 3.56 . \quad (1)$$

For the subsets of this data corresponding to only the feedings from one particular individual, the polynomial fit to all 42

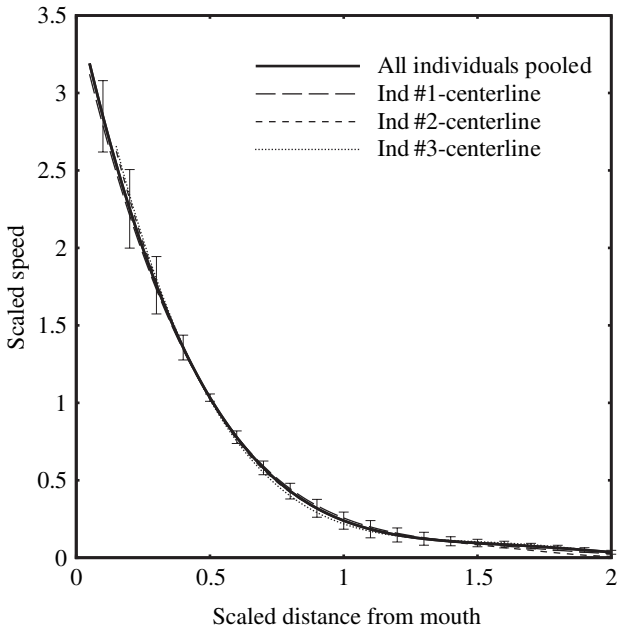

Fig. 4. Mean profiles of scaled speed along the centerline transect for each of the three individuals in addition to the polynomial fit to the pooled data set. SS_{pooled}=0.348x^4–2.49x^3+6.61x^2–7.78x+3.56. Error bars represent S.D. of the residuals about the fit lines. Note that all mean profiles fall within the error bars of the fit to the pooled data at all locations measured. Fluid speed at the mouth is somewhere between 3 and 4 times that at $\frac{1}{2}$ gape and fluid speed at a distance of 1.0 gape is approximately 0.25 the speed at $\frac{1}{2}$ gape.

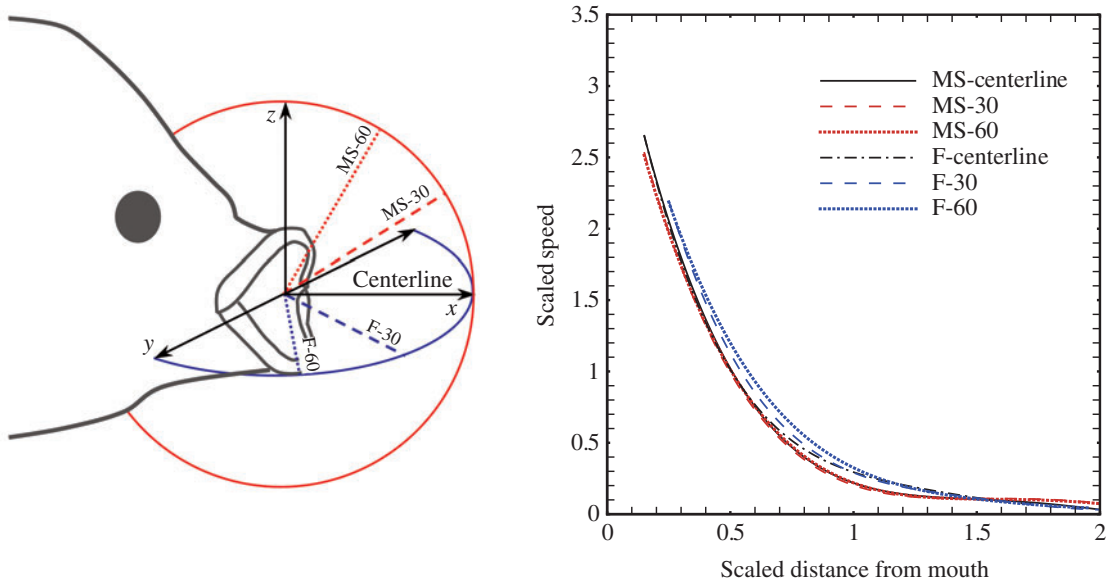

Fig. 5. Comparison of velocity profiles along the centerline and off-centerline transects within the mid-sagittal (MS-30 and MS-60) plane and frontal plane (F-30 and F-60) for individual #3. All transects share a common intersection at the center of the mouth opening. The region of significant fluid velocity induced by suction is constrained to a region close to the mouth. Note that the similarity between the velocity profiles shown in the mid-sagittal and frontal plane demonstrates that the distribution of velocity is essentially axi-symmetric, despite a laterally compressed fish body.

feedings, $SS_{pooled}(x)$, accounted for about the same amount of variation as the polynomial fit to only the feedings from that particular individual, $SS_{individual}(x)$. The r^2 of $SS_{pooled}(x)$ to the data subset consisting of feedings from a particular individual, r^2_{pooled}, was at least 99% of the r^2 of $SS_{individual}(x)$ to the same data subset, $r^2_{individual}$ (r^2_{pooled}=0.985 *vs* $r^2_{individual}$=0.986 for Ind#1, 0.986 *vs* 0.987 for Ind#2, and 0.975 *vs* 0.977 for Ind#3). Thus, the single functional relationship given in Eq. 1 was an effective description of the fluid speed in front of all individuals and the variation between individuals was small. The variation between the pooled and individual mean centerline profiles was within the S.D. of residuals about the pooled profile, as shown by the error bars in Fig. 4. The mid-sagittal and frontal planes share a common centerline, and the similarity between velocity profiles along the centerline (0°) and the off-centerline transects (30°and 60°) demonstrates symmetry of the flow field about the centerline axis of the fish (Fig. 5).

The cross section of the parcel of ingested fluid viewed in the mid-sagittal plane was an ovoid shape that was slightly taller than wide (mean height to width ratio=1.08±0.15), with an overall mean height 1.65±0.2 times that of peak gape, as shown for one feeding in Fig. 6. At the beginning of the strike, the prey was generally located at the center of the ingested volume of fluid. During the strike, jaw protrusion moved the mouth opening forward to a position near the original location of the prey, as shown in the inset to Fig. 6. Of the 30 feedings with a peak gape within ±2 mm of the mean (12.6 mm), the

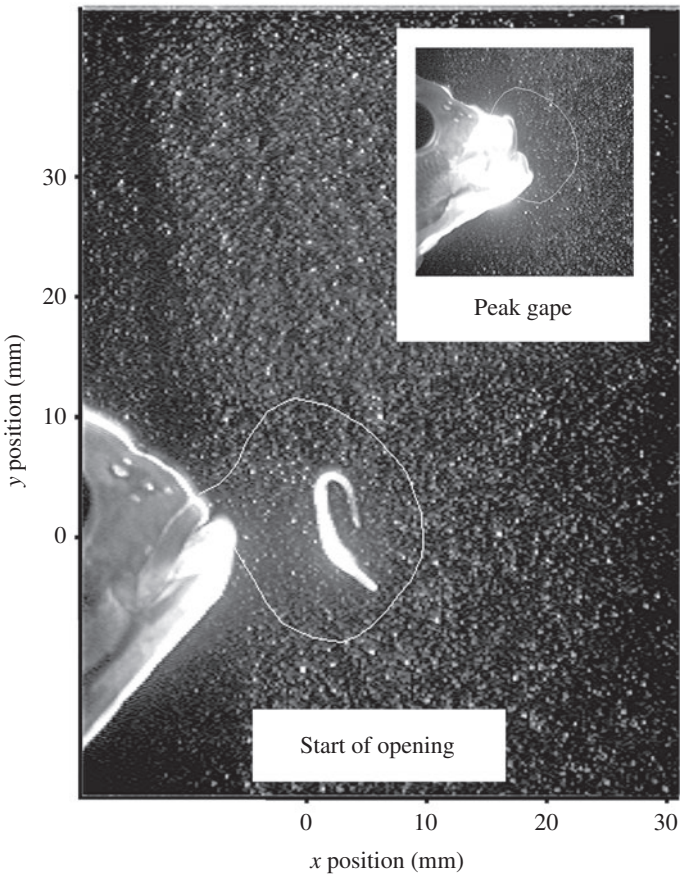

Fig. 6. Outline of the parcel of water ingested by the feeding fish during a suction-feeding event. All particles suspended within the white line were ingested during this strike. Inset shows the relative position of the fish at peak gape to the boundary of ingested fluid. Note the prey in the center of the parcel of water.

estimated volume of the ingested parcel ranged from 1800 to 6500 mm^3. This was equivalent to 0.7–2.6 times the buccal cavity volume of a bluegill with standard length of 15.1 cm, as estimated from silicone casts of a size series of 15 bluegill sunfish (D. C. Collar, unpublished dataset).

Temporal pattern

There was a general temporal pattern of generated fluid speed and key kinematic measures for all strikes, regardless of *TTPG*. $FS_{\frac{1}{2}PG}$ gradually increased and reached a peak value slightly before the time of peak gape and slightly lagging the time of peak protrusion speed (Fig. 7). The magnitude of fluid speed in the strike shown in Fig. 7B was larger than that of Fig. 7A both because *PG* was larger and *TTPG* was smaller. The relative timing of peak fluid speed to peak gape was not a function of *TTPG*, as the regression of time from 20% *PG* to peak fluid speed against time from 20% *PG* to 95% *PG* (*TTPG*) for all 42 feedings was not significant (P=0.25).

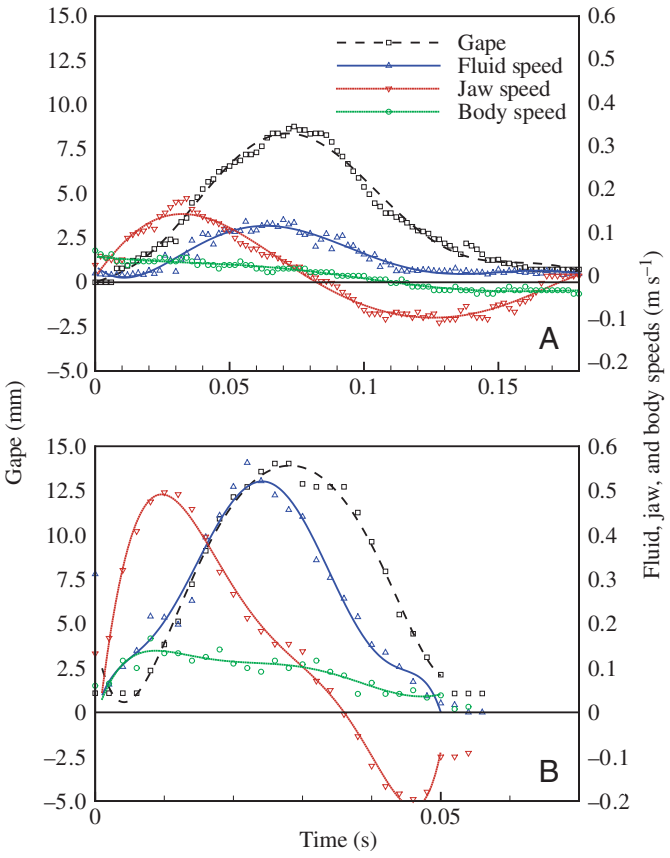

Fig. 7. Fluid speed compared to gape distance and ram speeds as a function of time for the two representative sequences. Fluid speed is located at a constant distance in front of the fish equal to $\frac{1}{2}PG$. (A) A relatively slow strike (*TTPG*=42 ms) and (B) a fast strike (*TTPG*=14 ms). Note the different *x*-axis scales for the two feedings. Although the magnitude of speeds and duration of events is different between the two, the relative timing is similar in that peak jaw speed precedes peak fluid speed, which in turn slightly precedes peak gape. Body ram speed continually decreases throughout the strike.

The general sequence of events was: start of opening, 20% opening, peak jaw speed, prey entering, peak fluid speed, 95% opening, and maximum jaw protrusion. Peak fluid speeds measured at three locations along the centerline transect all occurred nearly simultaneously with one another and with the time of 95% opening (Fig. 8). Prey capture generally began during mouth opening, at a time when peak jaw protrusion speed were near their maxima and fluid speed had not yet reached its peak. The mean time of the completion of prey ingestion was slightly before the time of peak fluid speed and 95% peak gape. Maximum protrusion occurred simultaneously with the time at which the mouth was open more than 95% of peak gape.

At any given scaled distance, higher fluid speeds were generated during faster strikes (Fig. 9). Peak fluid speed, $FS_{\frac{1}{2}PG}$, was principally a function of *TTPG* for each feeding (r^2=0.87) although some variation between individuals was apparent (Fig. 9).

Discussion

Our study presents data for a high-performance suction feeder (bluegill sunfish) over a moderate range of feeding behavior, as characterized by peak gape, *PG*, and time to peak gape, *TTPG*. The spatial pattern of flow generated by bluegill is constrained to a region close to the mouth. The area of significant fluid velocity forms a mushroom-shaped region extending unidirectionally away from the center of the mouth. This result confirms prior modeling (Muller et al., 1982) and empirical findings (Ferry-Graham et al., 2003) that fluid velocities are confined to a region within approximately one mouth diameter of the mouth aperture, and demonstrates the need for the predator to be able to locate its mouth very near the prey in order for suction feeding to be effective. Our data indicate a velocity profile that decreases as a function of distance from the mouth with a slope that also monotonically decreases as a function of distance from the mouth. In contrast to prior empirical studies (Ferry-Graham et al., 2003), we found no indication of a region of fastest fluid speed located at a distance anterior to the fish.

While both the prior (Ferry-Graham et al., 2003) and current studies used PIV and bluegill sunfish, there are numerous methodological improvements in the current study. The use of a higher frame rate (500 *vs* 250 Hz) leads to decreased particle displacement for a given fluid speed and use of a shutter (1/3000 s *vs* open shutter, 1/250 s) decreases particle streaking. Both of these allow for the measurement of higher absolute speeds, which is particularly necessary near the mouth. The use of a second mirror near the surface of the tank allowed for the illumination, and therefore measurements, of flow in the shadows of predator and prey. The use of validation schemes based on all neighboring points and interpolation of removed vectors, as was done in the previous study, is problematic near the fish because measured displacements are of the movement of the fish, not the fluid. The current validation scheme uses only neighboring points above and below, and therefore not

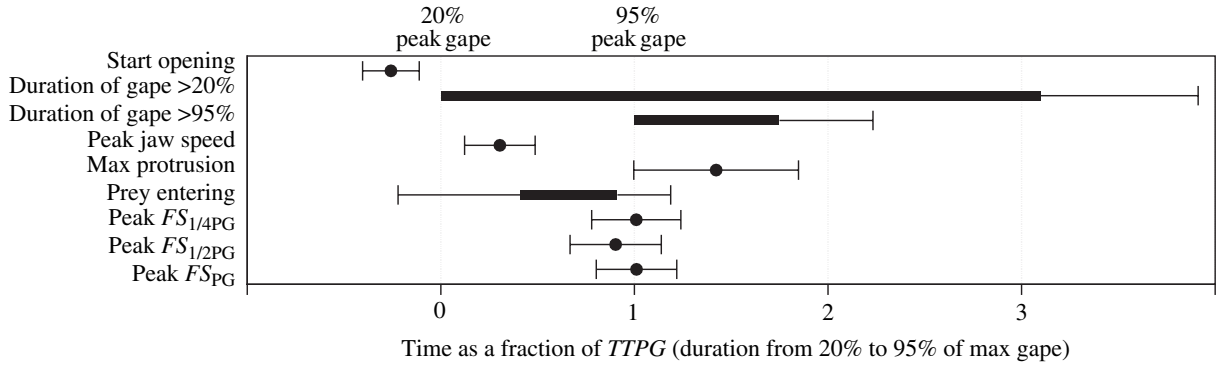

Fig. 8. Relative timing of kinematic events to measured peak fluid measured fluid speeds. To account for variation in absolute speed of the event, all times are shown normalized to *TTPG*. The time of each event is relative to the time of 20% opening and expressed as a fraction of the time from 20% opening to 95% opening (*TTPG*) so that both fast and slow strikes may be compared in the analysis. Because of the definition of *TTPG* used, the kinematic events of 20% *PG* and 95% *PG* are necessarily located at 0 and 1, respectively. All other symbols and error bars show the mean ± S.D. for all 42 feeding analyzed. Note that peak fluid speed occurs at approximately the same time as 95% opening, slightly preceding peak gape and peak protrusion. Events that have some duration, such as mouth opening more than 20% or 95% and the prey entering are represented as a filled bar with error bars (S.D.) for the start and finish of these events.

towards the fish and not in the direction of the gradient of velocity. Additionally, we did not replace measurements that were removed by the validation scheme.

A major finding of our study was a distinct spatial pattern of flow that was consistent for all feedings investigated in this study. After dividing spatial dimensions by the value of gape and the magnitude of fluid speed by the fluid speed at a fixed location in front of the fish ($FS_{\frac{1}{2}gape}$), this single functional relationship of scaled speed as a function of scaled distance from the mouth was shown to be accurate across the range of kinematic excursions observed in the study. Spatially, fluid velocity patterns scale with the size of the mouth aperture. While the spatial pattern of flow would likely be affected by variation in the shape of the mouth opening, it is thought that the pattern of fluid velocity presented here will be very similar in other suction feeders with similarly circular shaped mouths. It was also shown that the theoretical model for fluid speed along the centerline of the fish presented by Muller et al. (1982) is a good description of the measured speed. For scaled distances of 0.15 and greater, the polynomial fit and theoretical model are very similar to one another (Fig. 3B). As compared to the polynomial fit, the fluid speed and slope of the theoretical equation decrease with decreasing scaled distance at scaled distances smaller than 0.15. The polynomial fit has a maximum slope at the mouth aperture, whereas the theoretical curve has a slope of 0 at the mouth aperture. Empirical data are scarce in the area of discrepancy between these curves, so we cannot accept or reject either of these functions based on the current data set.

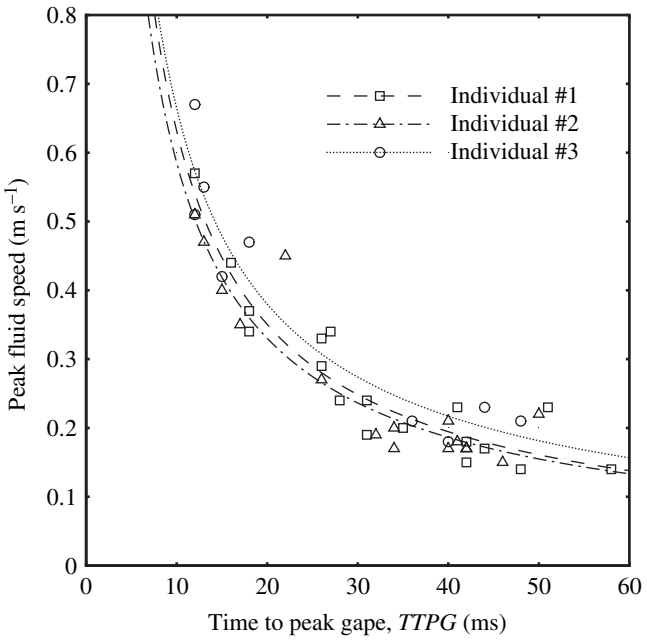

Fig. 9. DPIV data from 42 feeding sequences from three bluegill showing that time to peak gape (*TTPG*) is closely related to peak fluid speed (*FS*; measured at $\frac{1}{2}PG$ in front of the fish on the centerline), illustrating one mechanism of enhancing fluid speed during suction. Individual #1, peak $FS_{\frac{1}{2}PG}=4.6\times TTPG^{-0.86}$ ($r^2=0.86$); Individual #2, peak $FS_{\frac{1}{2}PG}=4.0\times TTPG^{-0.84}$ ($r^2=0.84$); Individual #3, peak $FS_{\frac{1}{2}PG}=4.2\times TTPG^{-0.80}$ ($r^2=0.92$); pooled data from all 42 feedings from three individuals, peak $FS_{\frac{1}{2}PG}=4.5\times TTPG^{-0.85}$ ($r^2=0.87$); speed, m s^{-1}; time, ms.

The fluid speed into the mouth is a function of the rate of change of volume of the mouth divided by the mouth aperture. The rate of change of volume is proportional to the square of gape and inversely proportional to *TTPG*. The area of the aperture is proportional to the square of gape, but independent of *TTPG*. These combined indicate that although absolute speeds (m s^{-1}) of kinematic movements are a function of both *TTPG* and *PG*, fluid speed is approximately independent of gape, but proportional to $TTPG^{-1}$. *TTPG* represents a combination of absolute speed of expansion and size of the gape that is directly relevant to fluid speed. A shorter *TTPG* necessarily corresponds to rapid kinematics. After dividing the absolute times of kinematic events and latencies between these

events by *TTPG*, the temporal pattern of fluid velocity, including the relative timing of peak fluid speed and key kinematic events, was shown to have a distinct pattern that is highly repeatable over the range of parameters investigated. The suction-feeding bluegill can enhance the magnitude of flow speed by increasing the rate of buccal cavity expansion, as indicated in our study by *TTPG*. After scaling the spatial pattern based on peak gape, approximately 87% of the variation in generated peak fluid speed was accounted for by time required for mouth opening, as quantified here with *TTPG*. While a first order approximation would predict that fluid speeds were proportional to $TTPG^{-1}$ (speed scales with the inverse of time), the empirical measurements of fluid speed suggest that fluid speed was inversely proportional to *TTPG* to an exponent less than 1 (range of 0.80 to 0.86 for the three individuals). This suggests a modulation of kinematic pattern of mouth opening that has some dependence on *TTPG*. Examples include a modulation of the timing of opening of the caudal valves that is correlated with *TTPG*, or decoupling of the anterior and posterior expansion, where posterior expansion is either slower or smaller in magnitude as a function of decreasing *TTPG*.

Peak gape and time to peak gape strongly affect the temporal and spatial patterns of flow. After accounting for the effects of these variables, there is a highly repeatable temporal and spatial pattern of flow. The consistent spatial and temporal patterns allow for the estimation of fluid velocities in front of a feeding bluegill based on relatively simple kinematic variables, *PG* and *TTPG*. This is a potentially powerful functional relationship, and if future interspecific studies confirm its generality across taxa the relationship would provide a unifying view of the behavioral and morphological diversity of suction feeders.

Drag forces experienced by a prey item that is positioned within a suction flow will be proportional to the square of fluid velocity, and therefore can be expected to fall precipitously as a function of distance from the predator's mouth opening. The decay of water velocity has been observed during suction feeding by fish using fluid visualization methods (Ferry-Graham et al., 2003), although the present study is the first to present a functional relationship for the decay of velocity based on empirical results. These results confirm the suggestions that velocity, and therefore forces that result from fluid velocity, are significant only in the region of approximately one mouth diameter in front of the fish. Because flow speed falls off so rapidly in front of the mouth, suction feeders gain little in terms of extending this flow field by even substantial increases in the fluid speed at the mouth opening. Instead, the chief advantage of increased flow speed at the mouth may be the increased magnitude of generated forces within the space very close to the mouth. The predator may extend the affected area of the flow field by opening the mouth wider, as we found the size of the velocity field to scale linearly with peak gape, and to extend the ingested volume further forward by using ram (Higham et al., 2005).

Fluid speed was not constant during the course of the feeding event. The time of peak fluid speed occurred only slightly before peak gape, and occurred simultaneously at three positions in front of the predator. The synchronization of fluid speed and gape is potentially a very effective feeding strategy because the bluegill simultaneously maximizes flow-induced forces acting on the prey and the space over which the forces occur. This result is in contrast to a model of the mouth as an expanding cylinder with no opercular slits, which leads to peak fluid speed very early in the expansion and a flow rate at the mouth aperture of zero at peak gape (van Leeuwen and Muller, 1984a). There are at least two mechanistic explanations for this. The first is that continued expansion of the posterior portion of the buccal and opercular cavities after peak expansion of the anterior portion prolongs the period of volumetric expansion of the total mouth past peak gape. A distinct delay in the posterior expansion (as measured by suspensory and opercular abduction) relative to gape was shown consistently throughout strikes of three species of *Lepomis*, including *L. macrochirus*, by Lauder (1980b) suggesting that the assumption of an evenly expanding cone or cylinder is not accurate. The anterior to posterior delay of expansion of major functional components of the head has been shown to hold true across a wide range of taxa (Lauder, 1982). The second is the possibility that the opening of the opercular slits allows fluid to continue to flow into and through the mouth, driven only by fluid momentum, after volumetric expansion of the buccal cavity has ceased. When the opercular slits are closed, the volumetric flow rate into the mouth aperture is exactly equal to the instantaneous volumetric expansion of the combined buccal and opercular cavities. After the opercular slits are open, this equality does not hold and the flow into the mouth is equal to the expansion of the mouth cavity, in addition to the volumetric flow rate out of the opercular slits. It is likely that both explanations contribute to the observed relationship.

The finding that peak fluid speed occurs at the time of onset of peak gape (as characterized by 95% PG) is also in contrast to expectations derived from more sophisticated models that link buccal expansion to fluid motion. The model of Muller et al. (1982), which allows for delayed posterior expansion and flow out of the operculum, was used to predict the temporal pattern of pressure and fluid speed within the mouth of four taxa (*Salmo*, *Esox*, *Gadus* and *Amia*; van Leeuwen and Muller, 1983). For the four species studied, the posterior expansion of the mouth cavity lagged the anterior expansion, beginning between 30% and 70% of *TTPG*. These simulations also allowed for opening of the opercular valves during buccal expansion, and the timing of this event was determined from kinematic data extracted from high-speed video for each species. The time of peak fluid speed at the mouth aperture predicted by the model ranged from 33% to 54% of the *TTPG* (data extracted from fig. 24 in van Leeuwen and Muller, 1983). This discrepancy in timing of fluid speed and mouth expansion between the model and empirical data presented here indicates that existing models are overly simplistic and do not account for subtleties in how fish actually manipulate water during

suction feeding. While the theoretical model has not been parameterized for *Lepomis*, we note that the rostral–caudal expansion wave, as characterized by simultaneous mouth opening and opercular expansion, has been characterized and is similar in *Lepomis* (Lauder, 1980b) and *Amia* (Lauder, 1980a). Given the similar kinematics despite significant morphological and phylogenetic differences between these two aforementioned species, we suspect that this kinematic pattern and resulting temporal relationship of fluid speed to kinematics may be characteristic of all suction-feeding fish.

Buccal casts of a size series of bluegill sunfish (D. C. Collar, unpublished data) show that the buccal cavity at peak expansion is fairly accurately described by a cylinder (posterior height equals 102% anterior height, posterior width equals 108% anterior width). The measurements of total ingested fluid volume presented here are as high as 260% of the buccal volume for a fish with the standard length of our specimens, as determined from these casts. It has been estimated that the total volume entering the head of a rainbow trout is 5.5 times the volume taken up before opening of opercular and branchiostegal valves (van Leeuwen and Muller, 1984a). This large additional volume is too large to be attributed to additional volume of opercular cavity and is therefore due to flow exiting the posterior portion of the mouth cavity through the opercular slits. By controlling the precise timing of mouth expansion and allowing flow to exit through the operculum during the feeding event, the suction-feeding fish is able to ingest a volume greater than the volume of the fully expanded head, which would be the maximum possible with no posterior valves.

Thanks to George Lauder for advice on setting up PIV for work with live fishes. This research was supported by NSF grants IBN-0326968 and IOB-0444554 to P.C.W. and A.Y.C.

References

Adrian, R. J. (1991). Particle imaging techniques for fluid mechanics. *Annu. Rev. Fluid Mech.* **23**, 261-304.

Aerts, P. (1990). Variability of the fast suction feeding process in *Astatotilapia elegans* (Teleostei, Cichlidae) – a hypothesis of peripheral feedback control. *J. Zool.* **220**, 653-678.

Aerts, P., Osse, J. W. M. and Verraes, W. (1987). Model of jaw depression during feeding in *Astatotilapia elegans* (Teleostei, Cichlidae) – mechanisms for energy-storage and triggering. *J. Morphol.* **194**, 85-109.

Carroll, A. M., Wainwright, P. C., Huskey, S. H., Collar, D. C. and Turnigan, R. G. (2004). Morphology predicts suction feeding performance in centrachid fishes. *J. Exp. Biol.* **207**, 3873-3881.

De Jong, M. C., Sparenberg, J. A. and DeVries, J. (1987). Some aspects of the hydrodynamics of suction feeding of fish. *Fluid Dyn. Res.* **2**, 87-112.

Drost, M. R., Muller, M. and Osse, J. W. M. (1988). A quantitative hydrodynamical model of suction feeding in larval fishes: the role of frictional forces. *Proc. R. Soc. Lond. B* **234**, 263-281.

Ferry-Graham, L. A., Wainwright, P. C. and Lauder, G. V. (2003). Quantification of flow during suction feeding in bluegill sunfish. *Zoology* **106**, 159-168.

Higham, T. E., Day, S. W. and Wainwright, P. C. (2005). Sucking while swimming: evaluating the effects of ram speed on suction generation in bluegill sunfish (*Lepomis macrochirus*) using digital particle image velocimetry. *J. Exp. Biol.* **208**, 2653-2660.

Lauder, G. V. (1980a). Evolution of feeding mechanism in primitive actinopterygian fishes: a functional anatomical analysis of *Polypterus, Lepisosteus and Amia*. *J. Morphol.* **163**, 283-317.

Lauder, G. V. (1980b). The suction feeding mechanism in sunfishes (*Lepomis*): an experimental analysis. *J. Exp. Biol.* **88**, 49-72.

Lauder, G. V. (1982). Patterns of evolution in the feeding mechanism of actinopterygian fishes. *Am. Zool.* **22**, 275-285.

Lauder, G. V. and Clark, B. D. (1984). Water flow patterns during prey capture by teleost fishes. *J. Exp. Biol.* **113**, 143-150.

Liem, K. F. (1973). Modulatory multiplicity in the feeding mechanism in cichlid fishes, as exemplified by the invertebrate pickers of Lake Tanganyika. *J. Zool.* **189**, 93-125.

Muller, M. and Osse, J. W. M. (1984). Hydrodynamics of suction feeding fish. *Trans. Zool. Soc. Lond.* **37**, 51-135.

Muller, M. and van Leeuwen, J. L. (1985). The flow in front of the mouth of a prey capturing fish. In *Fortschritte der Zoologie, Band 30 Functional Morphology in Vertebrates*, vol. 30 (ed. H. R. Duncker and G. Fleischer). Stuttgart W. Germany: Gustav Fischer Verlag.

Muller, M., Osse, J. W. M. and Verhagen, J. H. G. (1982). A quantitative hydrodynamical model of suction feeding in fish. *J. Theor. Biol.* **95**, 49-79.

Norton, S. F. (1991). Capture success and diet of cottid fishes – the role of predator morphology and attack kinematics. *Ecology* **72**, 1807-1819.

Norton, S. F. and Brainerd, E. L. (1993). Convergence in the feeding mechanics of ecomorphologically similar species in the Centrarchidae and Cichlidae. *J. Exp. Biol.* **176**, 11-29.

Nyberg, D. W. (1971). Prey capture in largemouth bass. *Amer. Mid. Nat.* **86**, 128-144.

Sanford, C. P. J. and Wainwright, P. C. (2002). Use of sonomicrometry demonstrates the link between prey capture kinematics and suction pressure in largemouth bass. *J. Exp. Biol.* **205**, 3445-3457.

Scarano, F. and Reithmuller, M. L. (1999). Iterative multigrid approach in PIV image processing with discrete window offset. *Exp. Fluids* **26**, 513-523.

Svanback, R., Wainwright, P. C. and Ferry-Graham, L. A. (2002). Linking cranial kinematics, buccal pressure, and suction feeding performance in largemouth bass. *Physiol. Biochem. Zool.* **75**, 532-543.

van Leeuwen, J. L. and Muller, M. (1983). The recording and interpretation of pressures in prey-sucking fish. *Neth. J. Zool.* **33**, 425-475.

van Leeuwen, J. L. and Muller, M. (1984a). A quantitative study of flow in prey capture by rainbow trout, *Salmo gairdneri*, with general consideration of the actinopterygian feeding mechanism. *Trans. Zool. Soc. London* **37**, 171-227.

van Leeuwen, J. L. and Muller, M. (1984b). Optimum sucking techniques for predatory fish. *Trans. Zool. Soc. London* **37**, 137-169.

Weihs, D. (1980). Hydrodynamics of suction feeding fish in motion. *J. Fish Biol.* **16**, 425-433.